

ALIGNMENT OF OFF-AXIS CONIC MIRRORS

Robert E. Parks

Optical Sciences Center, University of Arizona
Tucson, Arizona 85721

INTRODUCTION

The theory and practice of alignment of off-axis mirrors of conic section are discussed in terms of third order optics. The departure of a symmetric conic mirror from a sphere of the same vertex radius is derived. By a transformation of coordinates, this departure is applied to an off-axis section. It is shown that the off-axis section may be thought of as a surface containing astigmatism, coma, and spherical aberration when compared to a best-fit sphere. With this insight, we show how to determine the location of the optical axis when looking at the off-axis section from its center of curvature. Once this is known, the mirror may be placed in an autocollimation test and final alignment may be performed by observing the shape of the image.

The analysis is carried out in terms of Zernike polynomials. While their use is certainly not necessary and their formalism somewhat obscures the process at first, this same formalism affords great insight once a familiarity with these polynomials is gained.

While the analysis is carried through only the third order, it is perfectly straightforward (though tedious) to carry out the analysis for higher orders. More importantly, the third order analysis should give sufficient insight to permit the rapid alignment of very fast or grazing incident off-axis segments without resorting to higher order analyses.

DEPARTURE OF A SYMMETRIC CONIC MIRROR FROM ITS VERTEX SPHERE

We begin with the exact representation of the sag of a symmetric conic mirror, namely

$$z = \frac{c_v r^2}{1 + \left[1 - (\kappa + 1)c_v^2 r^2\right]^{1/2}} \quad (1)$$

Here the origin of coordinates is at the vertex of the mirror, r is the radial coordinate in the aperture, $c_v = 1/R_v$ is the vertex curvature, and κ is the conic constant of the mirror ($\kappa = 0$ for a sphere and $\kappa = -1$ for a parabola). If Eq. (1) is expanded in a power series, we have

$$z = \frac{r^2}{2R_v} + \frac{(\kappa + 1)r^4}{8R_v^3} + \dots \quad (2)$$

By subtracting the case for $\kappa = 0$ from the non-zero or conic representation, we obtain the departure of the conic from its vertex sphere

$$\Delta z = \frac{\kappa r^4}{8R_v} + \dots \quad (3)$$

to third order as illustrated in Figure 1.

DEPARTURE OF AN OFF-AXIS CONIC MIRROR FROM ITS BEST-FIT SPHERE

Consider the off-axis aperture in Figure 2 centered a distance h off axis with a pupil radius of a .

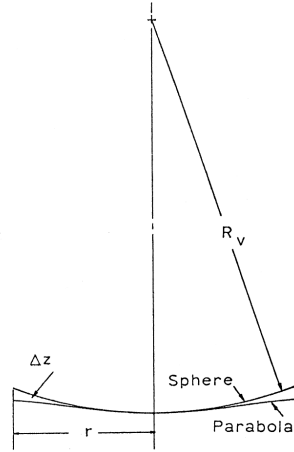


Fig. 1 Departure of parabola from Vertex sphere

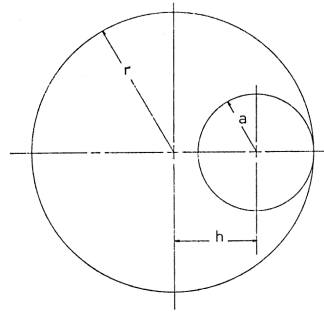


Fig. 2 Geometry of off-axis segment relative to symmetric paraboloid

While Eq. (3) is valid over all parts of the symmetric mirror, our interest is only in the departure over the off-axis section. In most cases, this is the only place where there will be any glass. To find the behavior of Δz over the off-axis pupil, the origin of coordinates must be shifted by h so that

$$\begin{aligned} x &= x' + h \\ \text{and} \\ y &= y' \end{aligned} \quad (4)$$

where the primed coordinates are centered about the vertex of the off-axis section. At the same time, we wish to perform the analysis over a normalized aperture so that Zernike polynomials may be used. This is done by letting

$$\begin{aligned} x' &= ax'' \\ \text{and} \\ y' &= ay'' \end{aligned} \quad (5)$$

where

$$x''^2 + y''^2 = \rho^2 \text{ and } 0 \leq \rho \leq 1 \text{ where } \rho \text{ is the radial variable of the Zernike polynomials.}$$

When the transformed variables are substituted in Eq. (3) we have

$$\Delta z = \frac{\kappa}{8R_v} [(ax''+h)^2 + (ay'')^2]. \quad (6)$$

Upon expanding this equation and equating like powers of x'' and y'' with those of the lower order Zernike polynomials (see Appendix), we find the coefficients of the polynomial terms to be

$$\begin{aligned} a_4^0 &= \frac{\kappa a^4}{48R_v^3} \quad (\text{spherical aberration}) & a_3^1 &= \frac{\kappa a^3 h}{6R_v^3} \quad (\text{coma}) \\ a_2^2 &= \frac{\kappa a^2 h^2}{4R_v^3} \quad (\text{astigmatism}) & a_2^0 &= \frac{\kappa(4a^2 h^2 + a^4)}{16R_v^3} \quad (\text{focus}) \\ a_1^1 &= \frac{\kappa(3ah^3 + 2a^3 h)}{6R_v^3} \quad (\text{tilt}) & a_0^0 &= \frac{\kappa(3h^4 + 6a^2 h^2 + a^4)}{24R_v^3} \quad (\text{piston}) \end{aligned} \quad (7)$$

and the sag over the off-axis aperture is

$$\Delta z = a_4^0 U_4^0 + a_3^1 U_3^1 + a_2^2 U_2^2 + a_2^0 U_2^0 + a_1^1 U_1^1 + a_0^0 U_0^0, \quad (8)$$

where the $U_n^{\pm m}$ are the corresponding Zernike functions. Clearly, the set of coefficients would be more symmetrical if we had also allowed an offset in the y direction for the off-axis pupil. Equation (8) can best be understood by considering it as a linear combination of six basis surfaces representing pure spherical aberration, coma, astigmatism, focus, tilt, and constant phase or piston.

In Figure 3, the upper left-hand picture shows the symmetrical mirror, an outline of the off-axis section at the middle right, and contour lines representing the departure between the symmetrical conic mirror and its vertex sphere. In the remaining pictures, just the off-axis section is shown along with contour lines of the departure over the pupil. Figure 3b is a representation of Eq. (8). It has exactly the same representation as the outlined section in Figure 3a except that it has been scaled to the diameter of Fig. 3a.

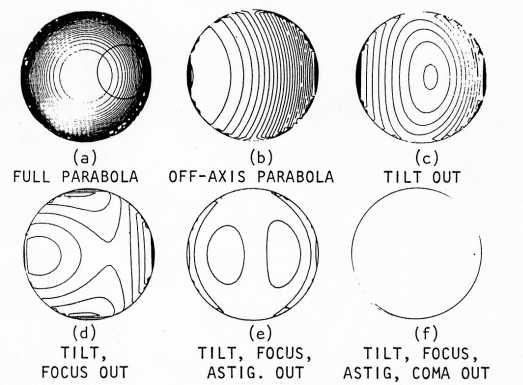


Fig. 3 Contour maps of off-axis segment from vertex sphere for various alignment conditions

If we think of the contour lines as interference fringes obtained by first looking at the symmetric conic at its center of curvature and then we place a mask over it so just the off-axis section can be seen, it is clear that if our interferometer is moved off the axis of the symmetrical mirror (in the minus x direction) or if we adjust the reference arm tilt mirror, we eliminate the "tilt" in Fig. 3b. This is what has been done in Figure 3c by setting the tilt and constant terms of Eq. (8) to zero. By further adjustment of the interferometer (away from the mirror) we could improve the out-of-focus condition. This is done analytically by setting a_2^0 to zero to produce Figure 3d. This picture represents the departure of the off-axis conic mirror from its best-fitting sphere. The center of curvature of this sphere does not lie on the axis of the symmetric parent mirror.

To third order, it is clear that the off-axis mirror surface consists of astigmatism, coma, and a small amount of spherical aberration, symmetric with the axis of the off-axis section. Since $h \geq a$ for an unobscured system, the ratio of astigmatism to coma will always be $3/2$ or greater ($a_2^2/a_3^1 \geq 3/2$), thus the mirror is more nearly pure toric the farther off axis and the slower it is. By the same reasoning, there will always be at least 8 times more coma than spherical aberration in the off-axis segment. All these departures scale linearly with the conic constant.

The balance of Figure 3 shows the shape of the departure from the best-fitting sphere if we first eliminate the astigmatism (by making the mirror toric or by bending) (3e) and then remove the coma (by polishing or perhaps alignment) (3f). In addition, by using some simple math and the coefficients, the required tilt and defocus are easily found for the best-fit sphere. Similarly, the differences in the astigmatic radii may be calculated to give an indication of the difficulty of manufacture of the off-axis section.

ALIGNMENT OF THE OFF-AXIS MIRROR, INITIAL STEP

In this section we consider the unfortunate situation in which the location of the axis has not been marked and the radius has not been given. From Figure 3d, it is clear that the axis could easily be located by viewing the surface from its center of curvature with an interferometer. The sharply rolled-down edge is farthest from the optical axis.

For any reasonably fast off-axis mirror, the aberrations will be so large that the whole surface will not be visible with the interferometer. From the form of the surface, it is clear from Eq. (7) that the ratio of astigmatism to coma will remain constant if the aperture of the mirror is stopped down and decentered so that the ratio $h:a$ remains constant. Thus the appearance of the surface will remain the same as that in Figure 3d. If the mask cannot be decentered sufficiently, the longer curvature axis of the astigmatism will lie along the radius of the symmetric asphere.

If an interferometer is not available, the orientation may be determined by looking at the image returned at the center of curvature. The shape of the image must be analyzed given the shape of the surface. To do this, we will make the simplifying assumption that the rays of light that form the image are normals to the surface. Of course, they are not, but if we place a point source on axis near the center of curvature of the off-axis segment, the rays will return to form a pattern of the same shape as that formed by the normals.

Now we need to determine where the normals intersect the j, k plane at a distance $(R_v + \delta)$ from the vertex of the off-axis segment. The coordinates of these intersections are (see Figure 4)

$$x_2 = x_1 - (z_2 - z_1) \frac{\partial z}{\partial x}$$

and

$$y_2 = y_1 (z_2 - z_1) \frac{\partial z}{\partial y}$$

where $z_2 = R_v + \delta$, $z_1 = \text{sag}$, and the partial derivatives are

$$\frac{\partial z}{\partial x} = \left(\frac{1}{a} \right) \left[a_4^0 (8U_3^1 + 4U_1^1) + a_3^1 (3U_2^2 + 3U_2^0 + U_0^0) + a_2^2 (2U_1^1) \right]$$

and

$$\frac{\partial z}{\partial y} = \left(\frac{1}{a} \right) \left[a_4^0 (8U_3^{-1} + 4U_1^{-1}) + a_3^1 (3U_2^{-2}) - a_2^2 (2U_1^{-1}) \right]$$

for the best fit departure (viz., $a_0^0 = a_1^1 = a_2^0 = 0$). Now by evaluating the Zernike functions $U_n^{\pm m}$ for a uniform grid over the normalized pupil $0 \leq \rho \leq 1$, we obtain the coordinates of the intersections of the normals or a simulation of the image. By varying the defocus parameter δ , we may see how the image varies with focus. Figure 5 is such an evaluation where 5b is a through-focus sequence of a typical set of parameters for an off-axis parabola ($R_v = 504$, $h = 40$, $a = 28$), while Figure 5a is the same for a segment of minimum possible decenter. The lower line in Figure 5c is for an extreme case of decenter. In all cases, we notice that the part of the image with the greatest intensity (highest density of dots) points toward the optical axis. Near the best focus position, the image appears much like a fish, the tail of which points toward the optical axis.

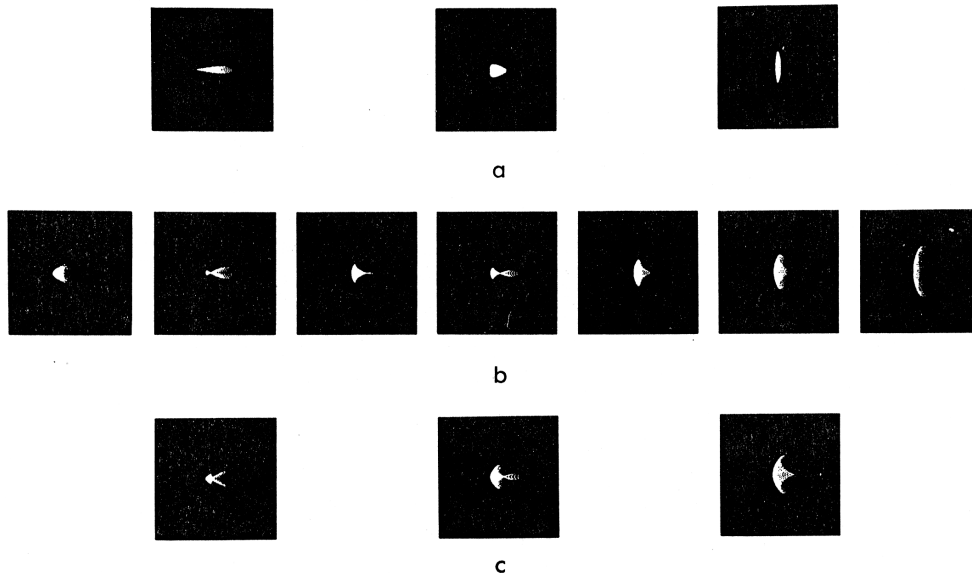


Fig. 5 Images produced by a point source placed near the center of curvature of an off-axis conic mirror for various amounts of defocus. (a) Images at minimum possible decenter while keeping

an unobscured aperture, (b) images for a typical decenter, (c) images for a large decenter. In all cases, the images at the left are inside focus (or closer to the mirror) and progressively go toward outside focus to the right. The optical axis is to the left (9 o'clock) in all cases.

While the above method allows the determination of the proper orientation of the off-axis segment, it does not do it with the kind of precision needed in an autocollimation test. A further refinement of the technique is the subject of the next section. It should also be pointed out in passing that if it is easy to create spot diagrams by simply playing with the Zernike coefficients, the opposite procedure is just as easy. The Zernike coefficients are just as easily found for Hartmann test data or any of the slope measuring tests such as Ronchi, wire, or lateral shearing interferometric tests.^{1,2}

ALIGNMENT OF THE OFF-AXIS MIRROR, FINAL STEPS

Once the off-axis section is set up for autocollimation as shown in Figure 6, the knowledge gained in the previous section will serve to establish a crude alignment. A first look at the image in autocollimation will reveal a large amount of astigmatism in an arbitrary orientation. What follows is the method to eliminate the astigmatism and simultaneously establish the location of the exact optical axis. First, the theory of what happens during the misalignment will be discussed.

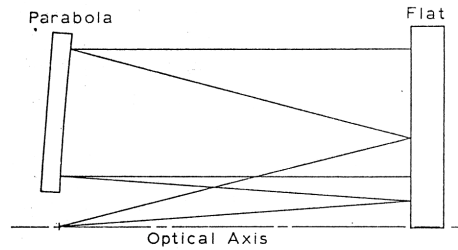


Fig. 6 Off-axis mirror segment being tested in autocollimation off a flat mirror

For any surface shifted from its properly aligned position, the change in the sag over the surface is just the slope of the surface in the direction of the shift times the amount of the shift. We have calculated the slopes in Eqs. (10), but we will rewrite them in a slightly different form to emphasize the type of aberration seen. (The first order effects have been dropped since they do not affect the shape of the image.)

$$\Delta sag_x = (8a_4^0 U_3^1 + 3a_3^1 U_2^2) \left(\frac{\Delta x}{a} \right)$$

and

$$\Delta sag_y = (8a_4^0 U_3^{-1} + 3a_3^1 U_2^{-2}) \left(\frac{\Delta y}{a} \right). \quad (11)$$

Using the coordinate system of Figure 7, the second part of Eq. (11) is equivalent to

$$\Delta sag_\theta = (-a_3^1 U_3^{-1} - 2a_2^2 U_2^{-2}) \Delta \theta. \quad (12)$$

We use this form because alignment may be easier to perform by rotating the segment about its mechanical center.

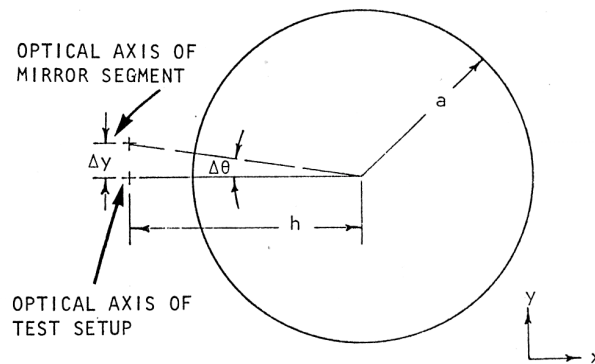


Fig. 7 Geometry of off-axis mirror alignment looking into pupil

Recalling that $a_4^\circ < a_3^1$, we see from Eq. (11) why astigmatism can be expected when the autocollimation test is set up. There will, in general, be a mixture of U_2^2 and U_2^{-2} due to misalignment in both the x and y directions. The small amount of coma present will decrease proportionately as the mirror is properly aligned.

The best procedure that we have found is to first eliminate the U_2^{-2} astigmatism term; that is, the astigmatism that appears oriented at an angle with respect to the coordinates of the test setup. This is done by adjusting in the y direction or about the center of the piece until the remaining astigmatism is lined up with the optical axis as illustrated in Figure 8a. Once this has been accomplished, a shift in the x direction will eliminate the remainder of the astigmatism. It may be necessary to iterate the procedure a second time to achieve an optimum alignment.

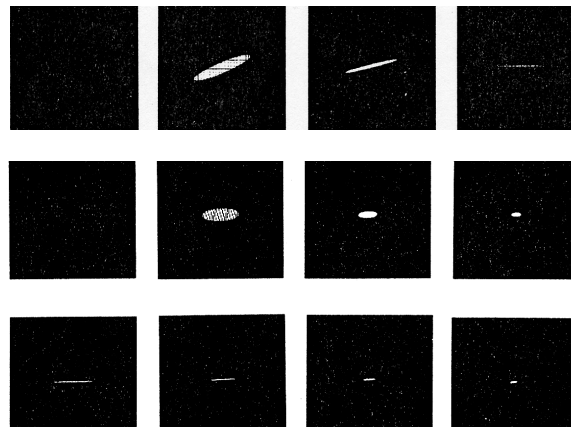


Fig. 8 Return images during alignment of off-axis segment autocollimation test.

Upper row of images – Progressive alignment in Δy or $\Delta\theta$

Middle row of images – Progressive alignment in Δx with slight defocus

Lower row of images – Progressive alignment in Δx with no defocus

Lastly, we point out that it may be nearly impossible to eliminate the astigmatism because it may be figure rather than alignment error. Equation (11) may be used to calculate the required additional decentration Δx and Δy to completely remove the remaining astigmatism in the test. If the remaining astigmatism is small, it may be more convenient to mathematically remove the astigmatism. This method is particularly appropriate if the off-axis segment is being polished or figured rather than being aligned into a system.

To mathematically find the residual surface or figure error in the off-axis segment minus any alignment error, set $a_2^2 = a_2^{-2} = 0$ and set

$$a_3^1 = a_{3initial}^1 - \frac{a_2^2 a}{3h}$$

and

$$a_3^{-1} = a_{3initial}^{-1} - \frac{a_2^{-2} a}{3h},$$

where the $a_{3initial}^{\pm 1}$ values are the coma coefficients derived from the interferometric test data.

When a contour map of the residual figure error is plotted, all low order coefficients through astigmatism are set to zero and the values for $a_3^{\pm 1}$ found in Eq. (13) are used for coma. All higher order coefficients are those found from the interferometric data.

CONCLUSION

A method to analyze the wavefront errors resulting from the misalignment of off-axis mirror sections has been presented along with a systematic method to use this analysis to find the proper alignment of such a mirror. The method is described in terms of the Zernike polynomials through the third order and can be considered exact only in the regime of third order optics. However, for small misalignments and as a guide for fast or grazing incidence optics, the method should be adequate.

ACKNOWLEDGMENTS

The help of coworkers Geraldine Wright, Nancy Davis, and Ker-Li Shu on portions of this paper is gratefully acknowledged. Gary Poczulp generated the contour maps and spot diagrams using the program FRINGE written by John Loomis. This work was partially funded under Air Force contract F29601-77-C-0073.

APPENDIX. ZERNIKE POLYNOMIALS

An expansion of a wavefront in Zernike polynomials has the general form³

$$W(\rho, \theta) = \sum_{n=0}^k \sum_{m=0}^n a_n^m U_n^m(\rho) [\cos(m\theta), \sin(m\theta)]$$

where $\rho = \sqrt{x^2 + y^2}$ for $0 \leq \rho \leq 1$, and the a_n^m are coefficients.

The $U_n^m(\rho)[\cos(m\theta), \sin(m\theta)]$ used in this paper are

$$U_0^0 = 1$$

$$U_1^1 = \rho \cos \theta = x$$

$$U_1^{-1} = \rho \sin \theta = y$$

$$U_2^0 = 2\rho^2 - 1 = 2(x^2 + y^2) - 1$$

$$U_2^2 = \rho^2 \cos(2\theta) = x^2 - y^2$$

$$U_2^{-2} = \rho^2 \sin(2\theta) = 2xy$$

$$U_3^1 = (3\rho^3 - 2\rho)\cos \theta = 3x^3 + 3xy^2 - 2x$$

$$U_3^{-1} = (3\rho^3 - 2\rho)\sin \theta = 3x^2y + 3y^3 - 2y$$

$$U_4^0 = 6\rho^4 - 6\rho^2 + 1 = 6x^4 + 12x^2y^2 + 6y^4 - 6x^2 - 6y^2 + 1$$

REFERENCES

- ¹ M. P. Rimmer and J. C. Wyant, "Evaluation of large aberrations using a lateral-shear interferometer having variable shear," *Appl. Opt.* 14, 142 (1975).
- ² N. H. Davis and T. A. Fritz, "Application of Zernike polynomials to reduction of wavefront-slope data," in *Optical Fabrication and Testing Workshop Technical Notebook*, Optical Society of America, 1980, pp. 39-42.
- ³ M. Born and E. Wolf, Eds., Principles of Optics (Pergamon Press, New York, 1975).

Copyright OSA. This paper was published in OSA Workshop on Optical Fabrication and Testing, N. Falmouth, MA as paper TuB4 (1980), and is made available as an electronic reprint with the permission of OSA. One print or electronic copy may be made for personal use only. Systematic or multiple reproduction, distribution to multiple locations via electronic or other means, duplication of any material in this paper for a fee or for commercial purposes, or modification of the content of the paper are prohibited. (This version of the paper has been reformatted and minor corrections of the original have been made 5/18/04.)